JGeope **2** *(1), 2012, P. 55-66*

X-Ray in-situ saturation monitoring, an aid to study relative permeability in water-wet carbonate rocks

Hamid Sharifi Galiuk*, Hessam Aloki Bakhtiari, Rezvan Behin, Mohammad Reza Esfahani
Core Research Dept., Center for Exploration and Production Studies and Research, Research Institute of Petroleum Industry, Tehran, I. R. of Iran
**Corresponding author, e-mail: sharifih@ripi.ir*
(*received: 21/05/2011 ; accepted: 23/05/2012*)

Abstract
The simultaneous flow of oil and water in porous media is described by relative permeability curves, mainly derived from laboratory experiments. Relative permeability is of paramount importance in predicting reservoir production performance and drive mechanisms and its value depends largely on the volume fraction of fluids present in the test samples. Nowadays X-ray scanners are one of the most accurate tools for non-destructive measurement of in-situ saturation. The mail purpose of this paper is to describe two-phase immiscible fluid flow behavior of low viscosity ratio oil/water through water-wet porous media interpreted by in-situ saturation profile data. Both steady state (SS) and unsteady state (USS) relative permeability measurement methods were applied and compared. The measured in-situ saturation profiles can confirm wettability character of studied rock samples and the yielded data are in good qualitative agreement with wettability characteristics of water-wet reservoir cores. In the USS experiments the saturation profile shapes characterize mainly production of oil before breakthrough and display front position. The flooding-rate dependency of the USS experiments was observed. In the SS experiments by imbibition process, water saturation in the samples was increased significantly even with flow of a very small fraction of water at the beginning of the test.

Key words*: Relative permeability; X-ray; In-situ saturation monitoring; Saturation profiles; Breakthrough.*

Introduction

The study of oil and water flow behavior in a reservoir rock needs accurate and representative relative permeability experiments and appropriate interpretation of the basic measured laboratory data. Relative permeability results and curve shapes are affected by many factors such as pore geometry, wettability of reservoir rocks, test fluids composition and viscosities, experimental technique and procedure, and fluids distribution.

Usually two distinct methods, namely unsteady state and steady state, are used for relative permeability measurements. USS displacement method is more popular than SS method. However, some researchers believe that SS techniques are the most reliable source of relative permeability data and provide more accurate data than USS methods (Maini *et al*., 1990).

For reservoirs with core-scale heterogeneity and mixed wettability, the SS laboratory tests are preferred (Edward *et al.,* 1981). Marcelo *et al.*, (2005) expressed that it is always advisable to have a good description of the pre-breakthrough relative permeability curves using an SS process, especially in light oil reservoirs where piston-like displacement often occurs.

Researchers infer the advantages and disadvantages of USS and SS methods of relative permeability measurements, but anyway, appropriate high quality relative permeability data is acquired during in-situ saturation measurement for both methods. The accuracy of relative permeability measurements depend largely on the accurate determination of fluids saturation. Conventionally the fluid saturations in the core samples are calculated by measuring the effluent fluids in the graduated vessels at ambient conditions or more accurately in the separators at test conditions; nevertheless the corrections for dead volumes are necessary. Nowadays, energy absorption techniques such as X-ray or gamma-ray are commonly used for measuring in-situ saturation in core studies (Maloney *et al*., 2002; Naylor *et al*., 1994).

The objective of conducted experiments was to distinguish the X-ray in-situ saturation profile shapes during low viscosity ratio fluids flow through water-wet rocks and to acquire representative relative permeability curves. For this purpose Unsteady State (USS) and Steady State (SS) experiments were performed on some carbonate cores.

Water saturation profiles obtained by X-ray scanner could be a basis for fluids flow processes in water-wet rocks. Because the experiments showed almost

the same characteristics of low viscosity ratio fluids flow in water-wet rocks, the results of only two typical plug samples, one from USS and one from SS experiments, were selected to be presented and discussed in this paper.

Phenomena and Process of Linear X-Ray Scanning

As it is stated in many related literatures (Maloney *et al*., 2002; Naylor *et al*., 1994), the principle of linear X-ray scanning is the attenuation of an incident X-ray beam with initial intensity of I passing through materials. This attenuation depends on the density of materials. From Beer-Lambert's law we have:

$$I' = I\, e^{-(\sum_{i=1}^{n} \mu_i x_i)} \qquad (1)$$

I': the intensity measured at the detector

μ_i: linear attenuation coefficient of material i

x_i: thickness of material i penetrated by the X-ray beam

n: the number of materials which are crossed by the X-ray beam

From 1980s, the linear X-ray scanning was widely used in the study of rock characteristics (Naylor, *et al.*, 1994). The X-ray scanning is a non-destructive measurement method of characterizing rock properties and fluids saturation in core samples.

Some advantages gained from the X-ray scanning of the core plugs in fluids flow studies are as follow:

- Produced volumes corrections (at conditions different from test conditions) are not necessary.
- In-situ saturation measurements are not affected by fluids emulsion or slow separation (Maloney *et al*., 2002).
- Local heterogeneities along the test samples, especially carbonate cores, are well recognized.
- In SS relative permeability measurements when the main core plug is between mixer and end effect reducer short plugs, in-situ saturation measurement is the only way to measure the core fluids saturation accurately.

For convenient application of this technique, fluids calibrations are necessary for further calculations of in-situ fluids saturation. The methodology is presented in detail in the appendix. It should be noted that the experimental conditions (confining and pore pressures and temperature), position of the core holder and the properties of the fluids in the core sample, and any material besides the fractions of test fluids within the X-ray beam path must be constant during all the stages of test and X-ray runs.

Reservoir Rock Samples and Fluids Characterization

Water-wet reservoir core plug samples (5 cm in length and 3.8 cm in diameter) of an Iranian carbonate reservoir were selected for this study. The test conditions, fluids properties and samples properties are presented in tables 1 and 2 Thin section study of sample S-6 showed a limestone with ooid grainstone with moldic porosity that causes low permeability with even high porosity of 28.882% and thin section study of sample S-3 showed a skeletal ooid grainstone dolomite with intra-particle and vuggy porosity.

Cross sectional CT scan images and porosity distribution along the selected samples are presented in figures 1 and 3 respectively. Pore size distribution and cumulative saturation curves of selected samples are shown in figure 2 Pore types of these samples are mainly in the range of meso (larger than 0.5μm) and macro (larger than 5μm). Sample S-6 has bimodal porosity.

The fluid system consists of simulated reservoir brine and n-Decane as the oil phase. The water was doped by adding 50 gr/Lit of KI salt to increase the contrast between oil and water X-ray absorption characteristics, yielding more accurate data. The oil-water viscosity ratio is 0.68 which confirms the stability of displacement process.

The experimental Setup

The key components of the setup include: X-ray generator and detector, composite carbon core holder, high pressure continuous/recirculation dual injection pumps, accumulators, a separator for measurement of effluent fluids, computer control and data acquisition system.

The X-ray generator and detector traverse the length of the loaded plug samples with the aid of a high precision motor. The X-ray beams are generated by applying a high voltage and are collimated to provide a spot diameter of 5 mm at the middle of the core plug, perpendicular to the flow direction. This linear X-ray in-situ saturation measurement method is a stop-measure-move technique. A precise measurement at each position takes approximately 30 seconds.

Table 1: Fluids properties and test conditions.

Confining pressure, psig: 4000	Pore pressure, psig: 2000
Temperature, °C: 90	Water salinity, gr/lit: 240
μ_W @ test conditions, cP: 0.59	Type of oil: n-Decane, μ_O @ test conditions, cP: 0.40

Table 2: Core samples properties undergone unsteady state (S-6) and steady state (S-3) tests.

Sample S-6	**Sample S-3**
Air permeability, mD: 9.628 Porosity, %: 28.882 Grain density, gr/cm^3: 2.71 Absolute water permeability (K_W), mD: 7.770 K_{base}, oil permeability @IWS, mD: 1.506 Constant flooding rate, cc/min: 0.10	Air permeability, mD: 248.40 Porosity, %: 23.418 Grain density, gr/cm^3: 2.84 Absolute water permeability (K_W), mD: 160.68 K_{base}, oil permeability @IWS, mD: 55.45 Constant flooding rate, cc/min: 2.50

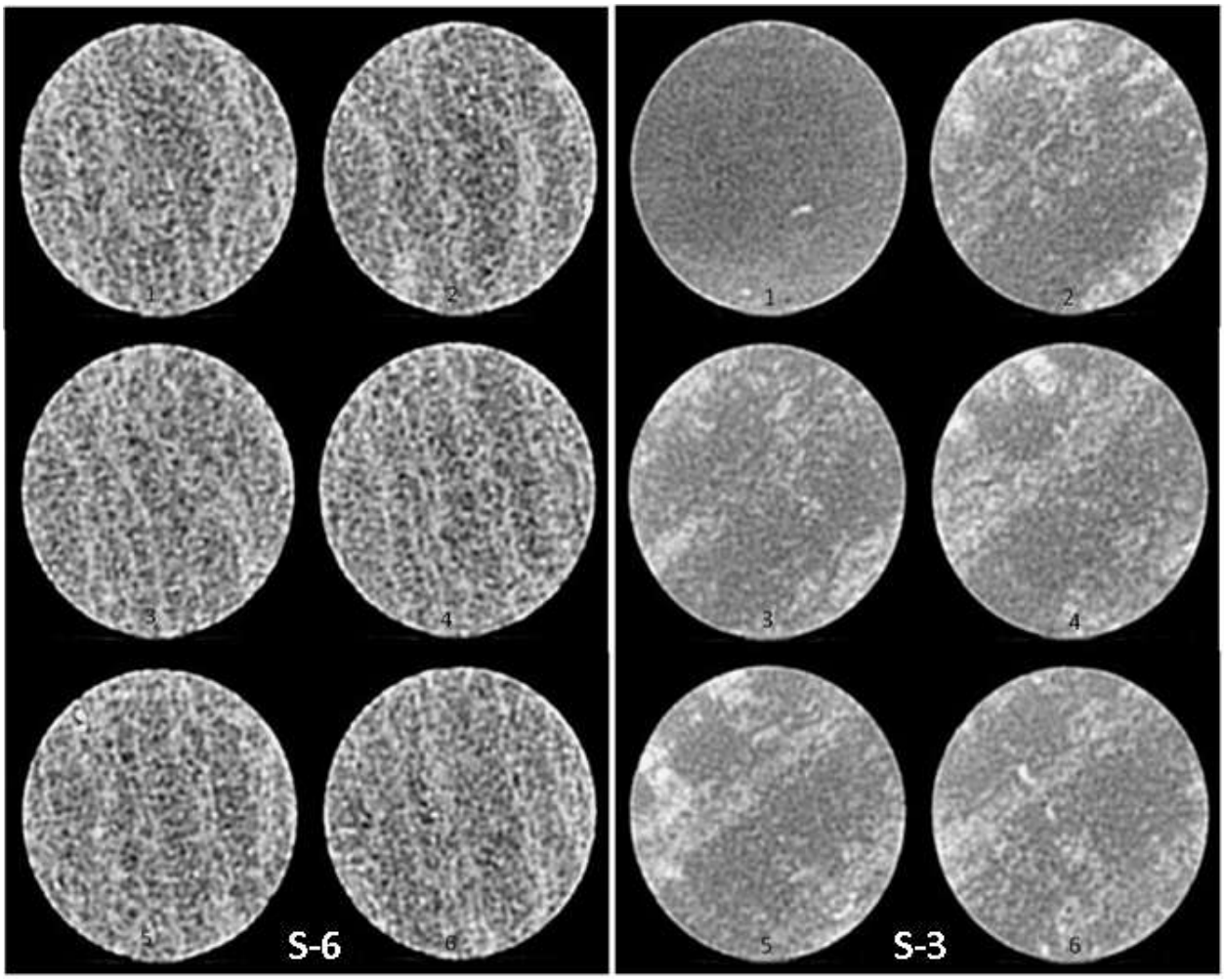

Figure 1: Selected cross sectional CT scan images of the samples (white to black: matrix to pore space)

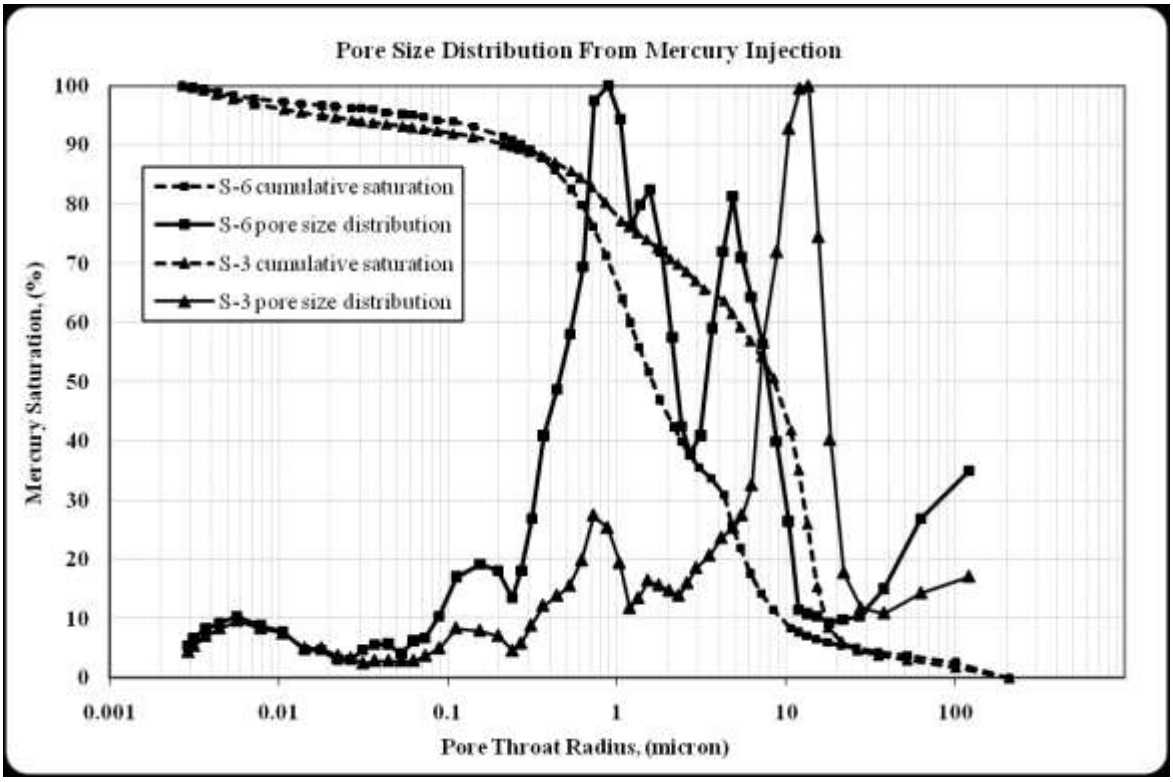

Figure 2: pore size distribution of samples S-3 and S-6.

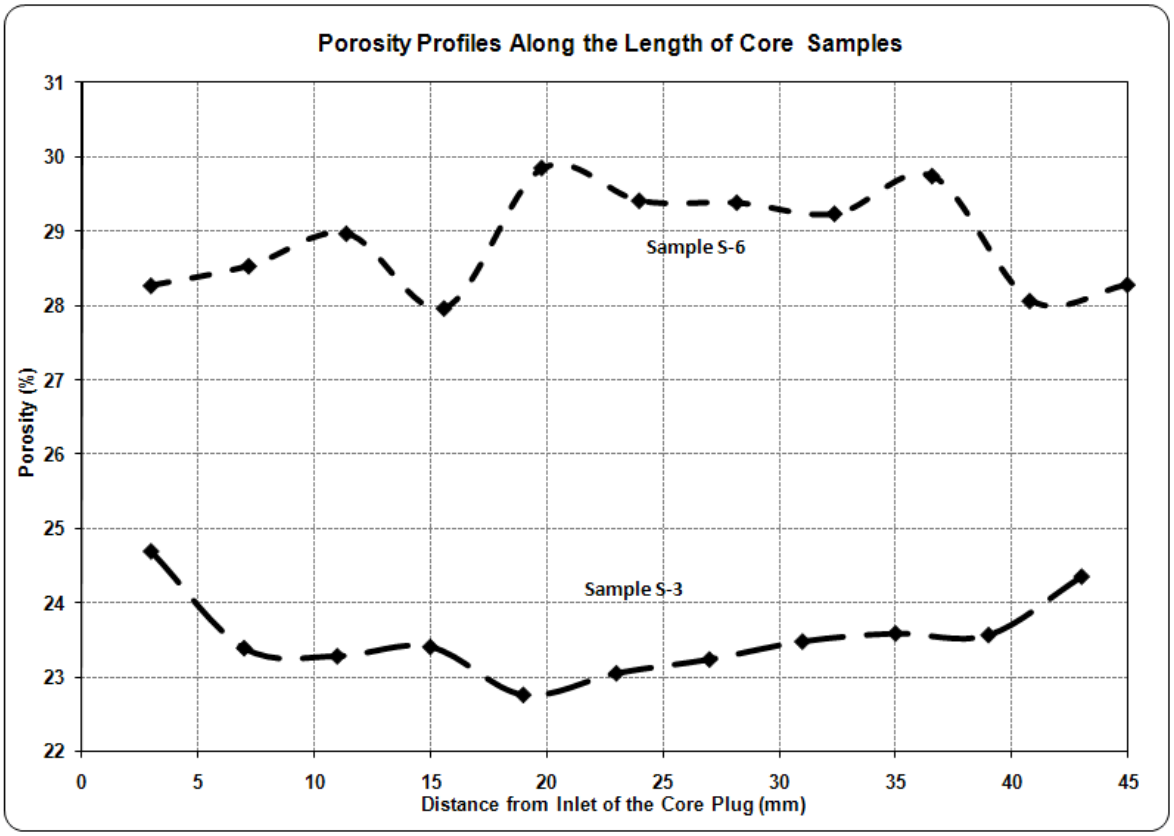

Figure 3: porosity distribution along the length of samples S-3 and S-6 obtained from linear X-ray scanner.

The Experimental Procedure

For performing a relative permeability experiment, a core plug was completely saturated with and immersed in simulated brine for at least 10 days to attain ionic equilibrium. The core plug was then loaded in the core holder and confining pressure of 4000 psig was gradually applied. The pore pressure was controlled by Back Pressure Regulator (BPR) set at 2000 psig. After reaching the equilibrium temperature of 90°C in the system, the absolute water permeability was obtained at different flow rates and water calibration X-ray runs were performed.

Irreducible water saturation was established by gradually increasing oil injection rate and by further injection of high oil flow in forward and backward directions 2 or 3 times repeatedly. After reaching the IWS condition, X-ray run was performed for calculation of IWS profile.

At the end of each experiment, the sample was washed to get completely saturated by oil. The procedure was injection of almost 15 pore-volumes of distilled water, methanol, toluene and oil respectively with gradually increasing the flow rates to an allowable rate for the core sample. Once the sample was fully oil-saturated at test conditions, the X-ray runs were performed for oil calibration.

With the aid of equations 4 and 7 in the appendix, the water saturation at any position along the sample and weighted average water saturation can be calculated. The repeatability of the X-ray data acquisition was checked through water and oil calibrations. It did not show any problematic noise.

Unsteady State Experiments: 2 accumulators, one filled with doped brine and the other one filled with oil were used to inject the fluids into the sample with a continuous dual injection pump. Neither mixer plug nor end effect reducer plug was used in USS experiments. Water-flooding experiments were performed with constant flow rate and the plug samples were continuously X-rayed.

At the end of the water-floods when oil production has ceased, as was indicated by consecutive X-ray runs and stabilized differential pressure; water flow rate was increased gradually to bump the oil phase. The end point water relative permeability at ROS was then measured.

The relative permeability values were obtained by using Jones & Roszelle (1978) graphical technique. For this purpose, the water saturation at effluent end face of the core plugs was measued by application of continuous X-ray runs during water-flooding process.

Steady State Experiments: Traditionally, SS experiments are performed by injecting two (or more) fluids through porous medium simultaneously. The average fluids saturation and the pressure drop across the core are measured at equilibrium conditions, practically when the saturation profiles and the pressure drop are relatively stable and inflow ratio of fluids equals the outflow ratio. The average core saturation from X-ray in-situ measurements along with the relative permeability values calculated directly with applying Darcy's law specifies one point on each of the relative permeability curves. For each plug sample, an appropriate total injection flow rate was chosen and by varying the rate fraction of the fluids, a sequence of relative permeability points was determined. The effective permeability to each fluid was directly determined from Darcy's law.

Ideally laboratory measurements of relative permeability should be representative of flow behavior in the reservoir. However using low flow rates in laboratory experiments presents several difficulties including: long test-time, low pressure drops which are difficult to be measured accurately, and experimental artifacts such as capillary end effect.

In an investigation, Chen and Wood (2001) concluded that measurements of imbibition relative permeability with SS method at flow rates typically used in the laboratory tests produce the same results as those obtained at flow rates representative of field rates. Therefore, the 2-phase SS relative permeability tests were performed with high enough total injection flow rates to overcome the influence of end-effect.

A total injection flow rate of 2.5cc/min was selected for sample S-3. Even high flow rates would not completely eliminate capillary end effects. Therefore very high permeable and porous short end-pieces were used at the inlet and outlet ends of the plug samples, one to act as a mixer and the other one to eliminate the end effect respectively. The lithology of these plugs (2.5 cm long) was carbonate from the same reservoir cores.

Results and Discussion

The unsteady state and steady state experiments

yielded the same characteristics of low viscosity ratio fluids flow through water-wet porous media. Hence typical results of one USS and one SS test are presented and interpreted in this paper. The error analysis was performed according to equation 9 in the appendix and resulted accuracy of 1% in in-situ saturation measurements.

During irreducible water saturation establishment significant end effect was present in the samples. Although we increased the oil flooding rate in order to reach true and uniform IWS profile, no significant changes were observed in shape of saturation profiles and the value of average IWS (Fig. 4 and 8). Therefore, with some modifications in the apparatus the oil was injected in forward and backward directions repeatedly. However, the IWS profile of sample S-6 shows existence of end effect that holds up the water saturation up to 40% at the effluent end of the core plug. The IWS in sample S-6 was checked by volumetric measurement that was approximately 35%, which approaches to average IWS from X-ray, but distinction of X-ray data was to exhibit circumstance of water saturation distribution along the core length and perception of this data.

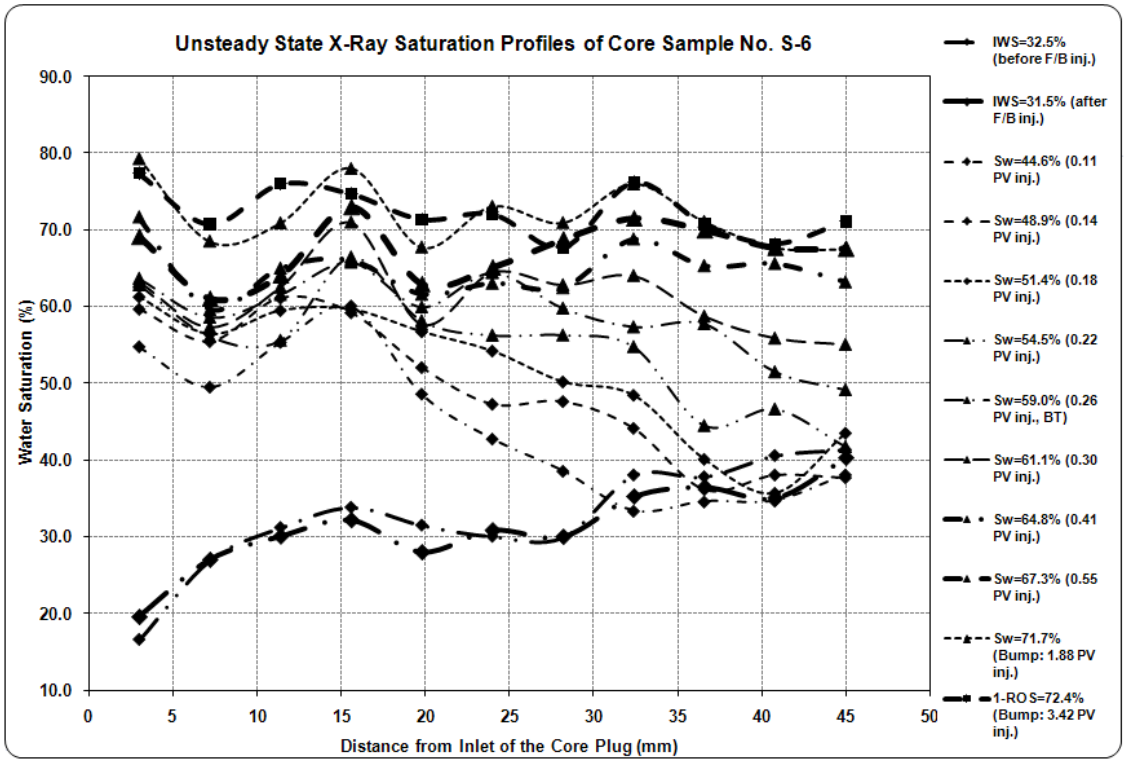

Figure 4: In-situ water saturation profiles during unsteady state low viscosity ratio experiment through naturally water-wet porous media, sample S-6.

The saturation value of non-wetting oil phase is controlled by reservoir rock wettability characteristics. The average IWS value determined by X-ray in-situ saturation data was high as expected in a water-wet rock. When non-wetting phase tries to enter to the wetting phase, due to snap-off, the non-wetting phase becomes discontinuous globules through the wetting phase.

Unsteady State Experiments: Since average and core end-face water saturations were measured directly from X-ray in-situ saturation data, no correction is needed to compensate for upstream and downstream tubing volumes and time lag between when fluids exit the core and when observed. In addition, we applied low constant injection rate and knowing the saturation difference between two measurement profiles, the drained oil volume and therefore the volumes of produced fluids could be calculated.

The saturation profiles before breakthrough and after that are presented in figure 4. The IWS profile before forward/backward injection shows end effect. After forward/backward injection, water

saturation was just decreased 1% and end effect was not much eliminated which shows very high water tendency of the core.

The saturation profile shapes characterize mainly production of oil before breakthrough and display the displacement of front position. Figure 6 shows the variation of differential pressure with time during water-flooding and bumping and Figure 7 displays oil production versus pore-volumes of injected water. Differential pressure increased sharply until BT and after reaching its highest value decreased gradually. This indicates smooth decrease of trapped oil droplets along the paths of water flow in the core, and due to water wetting tendency of porous media, water injection became convenient and differential pressure decreased smoothly.

The saturation profiles after BT tend to be uniform. The relative permeabilities to water and oil versus water saturation, shown in figure 5, are in qualitative agreement with wettability characteristics of water-wet reservoir cores and Craig's (1971) rules of thumb. Both Corey (1954) and LET (Lomeland *et al*., 2005) models were fitted to data. Water saturation was 52% at cross-over point, oil recovery at breakthrough was 40% of oil initially in place (OIIP) and 67% of recoverable oil, and this amount of oil was swept by 0.26PV of injected water.

The mobility ratio, which is defined as (Krw/μw)/(Kro/μo), is a dominant parameter for frontal stability in oil displacement by water. The end-points mobility ratio of sample S-6 (0.32) indicates a favorable displacement. In displacement of light oils by water encroachment, the breakthrough happens when oil saturation is near to residual value and after BT a little oil is produced and this evidence is proved by uniform saturation profiles after water BT. Only 12% of OIIP was recovered after BT and this happening is evidence of mainly oil production before BT in water-wet rocks. A large fraction of this 12% OIIP could have been remained due to rock sample heterogeneity.

In USS relative permeability experiments the inlet part of flooded core reaches its residual oil saturation value sooner than its outlet part and the bump flow is performed to diminish the end effect. Comparing the last saturation profile of flood (0.51PV injected) and the one for bump (3.42PV injected) of sample S-6 in figure 4 indicates production of almost 10% of oil during bump flow from the inlet part of plug sample S-6. This can be interpreted as highly flooding-rate dependency of USS relative permeability experiments especially in heterogeneous porous media.

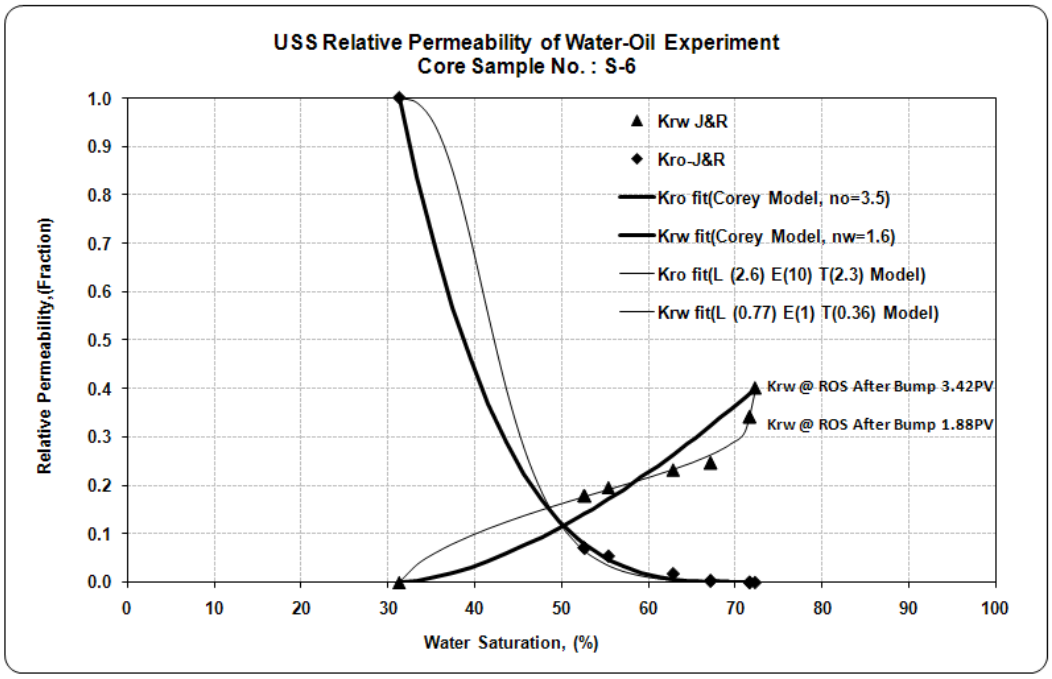

Figure 5: Relative permeability to water and oil obtained from unsteady state experiment performed on sample S-6 and fitted models.

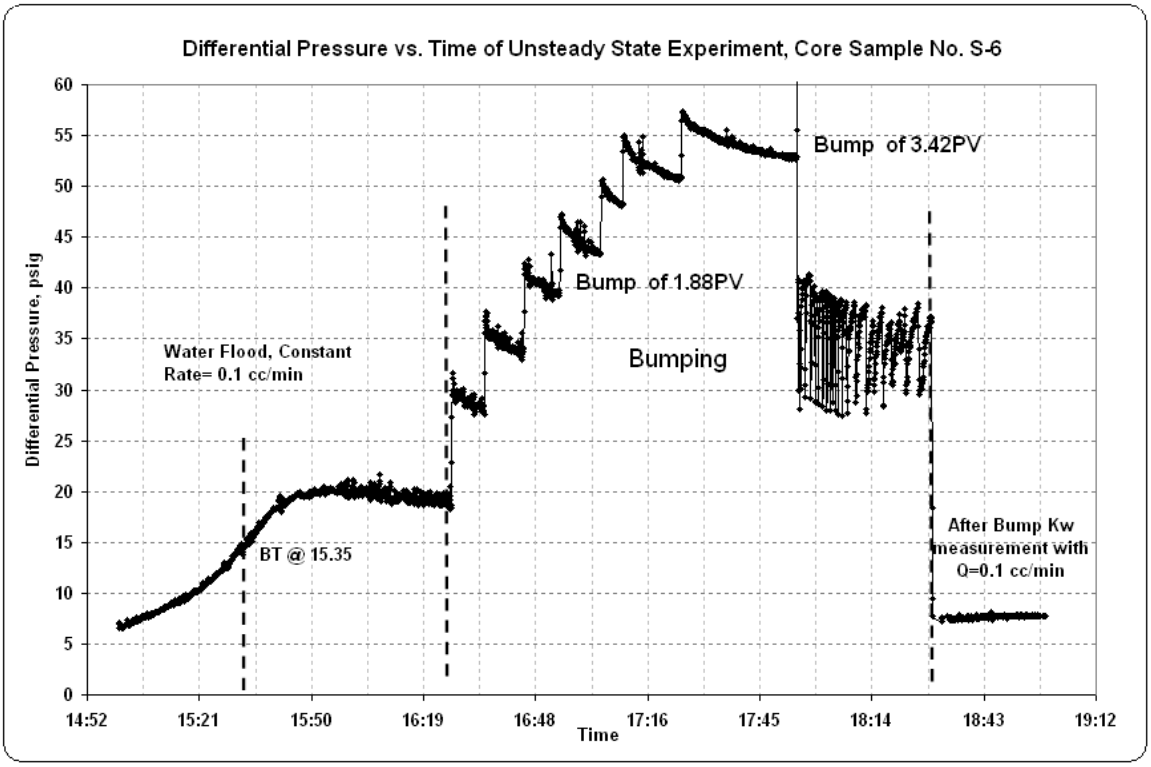

Figure 6: Recorded differential pressure during water flooding and further bump performed on sample S-6.

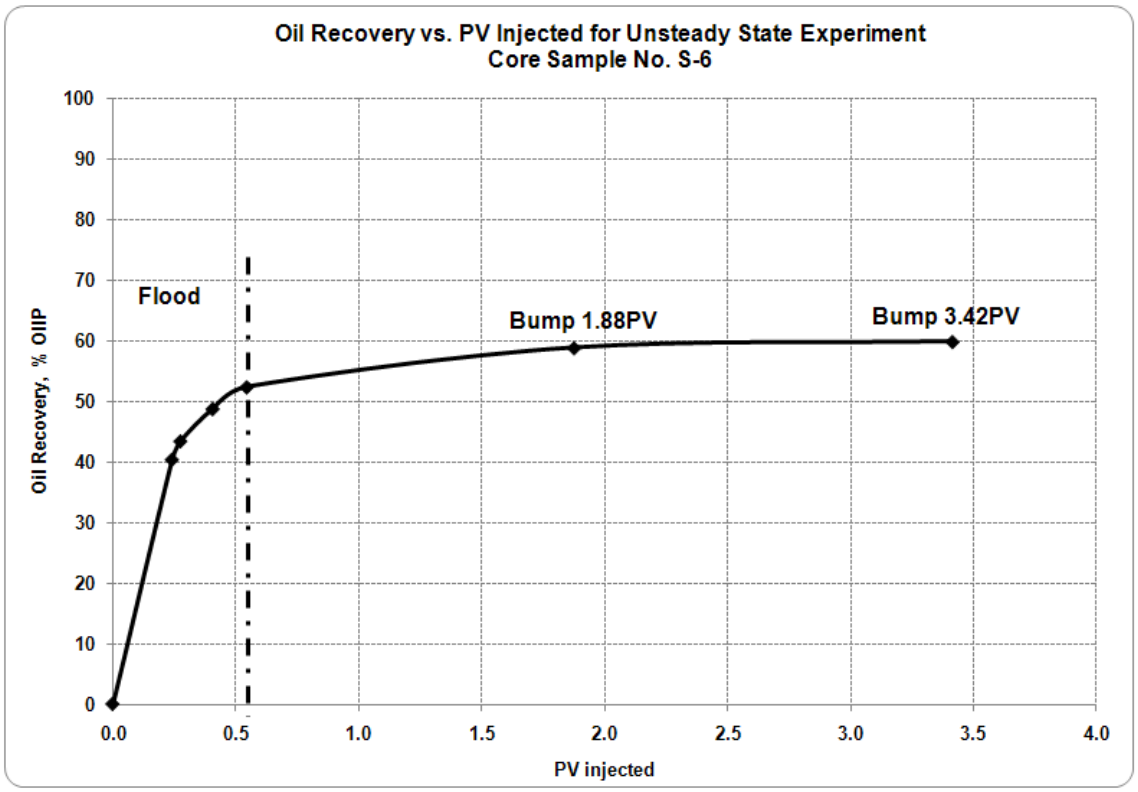

Figure 7: Oil recovery (%OIIP) during water flooding and further bump performed on sample S-6.

Steady State Experiments: The imbibition process, which means gradually increasing water fractional flow, was applied on sample S-3. Water fractional flow of 10% of total injection rate was selected as the first stage of oil and water co-injection to sample S-3. Its corresponding water

saturation profile located much upper than IWS profile. This event was observed in SS experiments with even a lower water fractional flow of 2% in other test samples.

Even though the water fractional flow was increased from 23.3% to 100%, the average water saturation in the core plug increased just 5%. This indicates that the applied oil flow rates might have been flowing through large pore throats of the core and due to water wetness most of pore spaces have been occupied by water and the core expels most of the oil flowing through it.

The end effect is obvious from IWS profile before forward/backward injection and after that end effect was eliminated but not completely (Fig. 8). From water fractional flow of 36.7% to 76.7% the average water saturation did not change or if any change occurred have not been in the precision range of the apparatus. In order to reach true ROS, the flow rate was increased twofold, but no considerable oil was produced. Despite what happened in low flow rate water-flooding of sample S-6, the water injection rate at end-point (Krw at ROS) has been high enough that saturation profile at bump flow is almost the same as without bumping. The saturation profiles are uniform and exhibit elimination of end-effect as a result of existing end-effect reducer short plug, and selecting high enough total injection flow rate.

The oil relative permeability curve shows a sudden decrease at the stages after 23.3% of water fractional flow which is an evidence of highly water-wetness of the core plug (Figure 9). The cross-over point is at 68% of water saturation and measured end-point Krw at ROS is 0.22. The relative permeability curves are in good agreement with wettability characteristics of water-wet reservoir cores and Craig's (1971) rules of thumb. Both Corey (1954) and LET (Lomeland et. al., 2005) models were fitted to experimental Krw data but due to S-shape of Kro data only LET model was fitted to Kro data.

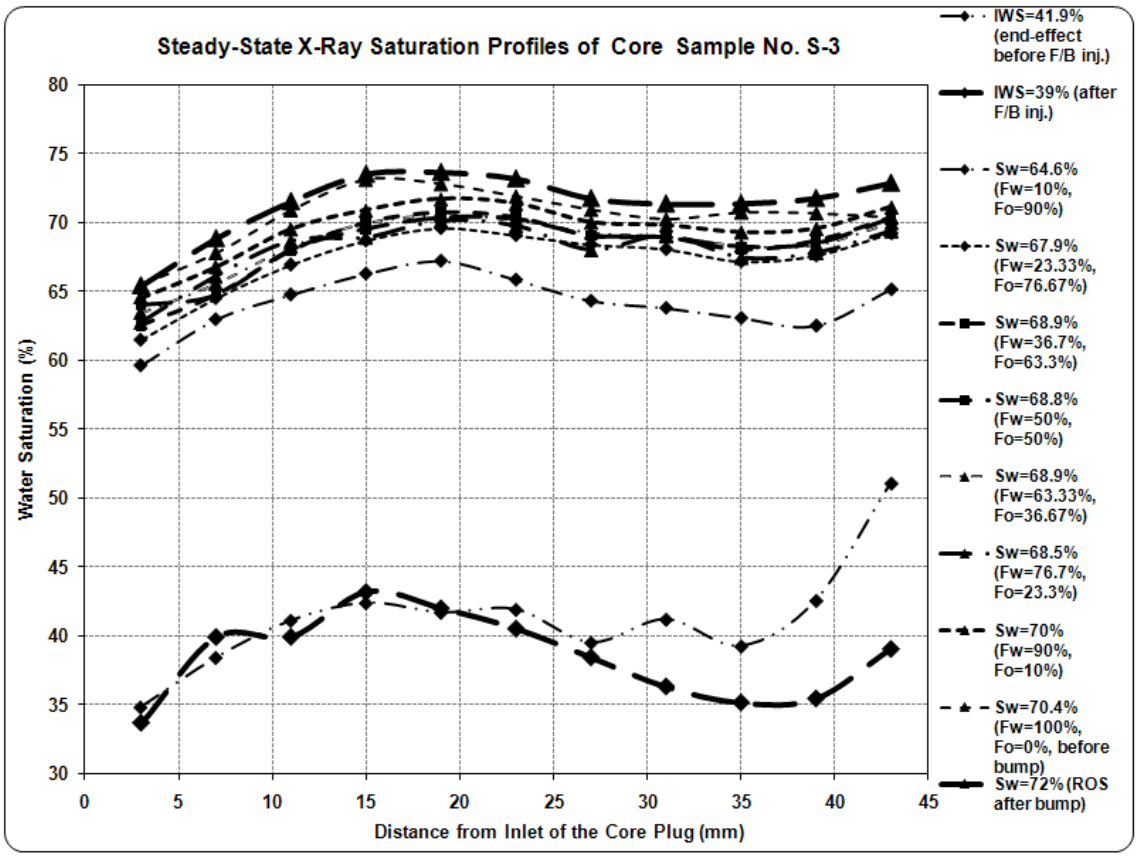

Figure 8: In-situ water saturation profiles during SS low viscosity ratio experiment through water-wet core performed on sample S-3. F_W and F_O are water and oil fractional flows.

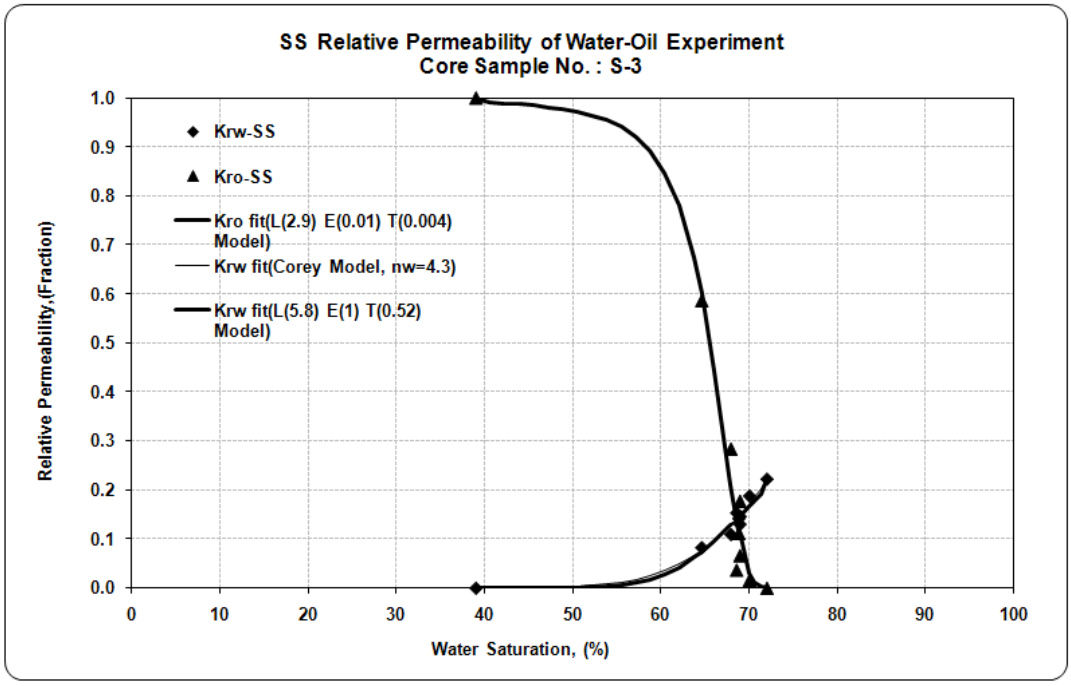

Figure 9: Relative permeability to water and oil obtained from steady state experiment performed on sample S-3 in 6 steps and fitted models.

The linear X-ray in-situ saturation measurement method is a stop-measure-move technique. Hence, for USS experiments some time lag corrections were applied and in high flooding rate experiments, this technique can only measure outlet saturation changes, and does not give reliable saturation profiles for overall core length. Therefore the saturation profile results in SS measurements are more accurate than USS ones, since the measurements are performed at equilibration conditions.

Conclusions

The following conclusions can be inferred from this investigation:

The X-Ray in-situ saturation is perceptible technique for characterizing the specifications of relative fluids flow through porous media. The in-situ saturation profiles can confirm the fact that wetting and non-wetting phase saturations are controlled by reservoir rock wettability characteristics.

The error analysis was performed and resulted accuracy of 1% in in-situ saturation measurements.

In low viscosity ratio water-oil displacement processes, the breakthrough occurs when the oil saturation is near to residual value; resulting production of a large fraction of recoverable oil in place before BT. Although the core sample S-6 was heterogeneous, 67% of recoverable OIIP was swept before BT.

Although it is always advisable to perform SS experiments to have a good description of pre-breakthrough relative permeability curves, in low viscosity ratio oil-water SS experiments in water-wet rocks, very low fraction of water injection largely increases water saturation in the core, which was visualized by X-ray saturation profiles. It is due to high tendency of rock to detain water, even when a very low water fraction is flowing through the core.

The saturation of non-wetting oil phase was controlled by reservoir rock wettability characteristics. During the process of IWS establishment, the amount of immovable water in the core plugs was high because of oil snap-off. Even though oil was injected with high flow rates to the core plugs in forward and backward directions repeatedly, the end effect was not completely eliminated.

Long or composite cores are highly recommended to be used for relative permeability experiments which effectively reduce the end effect. However with the aid of in-situ saturation profiles, the unaffected zone of core samples can be used for relative permeability calculations, provided that corresponding differential pressures can be measured.

Acknowledgments
The authors would like to place on record, their appreciation for the support rendered by Research and Technology Directorate of National Iranian Oil Company, on the research leading to the present article. The authors also acknowledge with grateful thanks the support from Dr. Kazemzadeh, the head of Reservoir Engineering Department of RIPI.

Appendix
The methodology of two-phase fluids saturation measurement by this system in any L_x position of a core sample is presented.

$$I_W = I\, e^{\sum(-\mu_m x_m)-\mu_W x_t} \quad (1)$$

$$I_O = I\, e^{\sum(-\mu_m x_m)-\mu_O x_t} \quad (2)$$

$$I_{WO} = I\, e^{\sum(-\mu_m x_m)-\mu_W x_W-\mu_O x_O} \quad (3)$$

I: the constant incident beam intensity of a level of energy in the X-ray system I_W: fully water-saturated core
I_O: the intensity of a core plug fully saturated with oil measured by the detector
I_{WO}: the measured intensity of a beam passing through a core plug which is partly saturated with water and partly saturated with oil during the experiment
$\sum(-\mu_m x_m)$: total attenuation of X-ray beam caused by the constant materials containing the core holder, confining oil and rock matrix within the beam path during every stages of the experiment
μ_W and μ_O: the linear attenuation coefficients of water and oil respectively
x_t, x_W and x_O: total thickness of fluids penetrated by the X-ray beam, partly by water and partly by oil
Total thickness of fluids is total effective pore space at each slice of the plug sample being X-ray scanned and the fraction of each fluid to total void space is its saturation fraction.
From equations (1) to (3) one can do the following calculations (Maloney, 2002):
Whereas: $\boldsymbol{x_t = x_W + x_O}$

$$Ln\left(\frac{I_{WO}}{I_O}\right) \Big/ Ln\left(\frac{I_W}{I_O}\right) = \frac{-\mu_W x_W-\mu_O x_O+\mu_O x_t}{-\mu_W x_t+\mu_O x_t} = \frac{-\mu_W x_W-\mu_O (x_t-x_W)+\mu_O x_t}{(\mu_O-\mu_W)x_t} = \frac{x_W}{x_t} = S_W \quad (4)$$

S_W is in fraction and is obtained at each slice in the core plug sample penetrated by the X-ray beam. Equation (4) shows that we do not need to obtain the attenuation coefficients of the materials any more. Having the bulk porosity of the sample (φ_{Bulk}), the porosity (φ_i) at i[th] position along the sample is calculated from the equations in below:

$$\varphi_i = \varphi_{Bulk} Ln(\tfrac{I_O}{I_W})/Avg \quad (5)$$

$$Avg = \textstyle\sum_{i=1}^{n} Ln(I_O/I_W)/n \quad (6)$$

There are n positions along the plug sample which have been X-rayed.
The weighted average water saturation with accounting porosity changes along the heterogeneous core samples is calculated from the following formula:

$$Sw_{ave} = \frac{\sum(Sw_x * \varphi_x)}{\sum \varphi_x} \quad (7)$$

In order to obtain the uncertainty of two-phase fluid saturation measurement, from equation (4) we know that calculated water saturation is a function of I_W, I_O and I_{WO}.

With differentiating equation (4) with respect to each of the above variables, one can get the following equation which is sum of the squares of the individual errors in S_W:

$$dS_W^2 = [\tfrac{\partial S_W}{\partial I_W} dI_W]^2 + [\tfrac{\partial S_W}{\partial I_O} dI_O]^2 + [\tfrac{\partial S_W}{\partial I_{WO}} dI_{WO}]^2 \quad (8)$$

In the equation (8), $dS_W, dI_W, dI_O, and\ dI_{WO}$, are absolute errors in S_W, I_W, I_O, $and\ I_{WO}$ respectively. The absolute errors of the measured intensities at different stages of the experiment can be obtained by statistical analysis of a large number of the intensities measured at a random position of core sample.

References

Maini, B., Coskuner, G., Jha, K., 1990. A Comparison of Steady-State and Unsteady-State Relative Permeabilities of Viscous Oil and Water in Ottawa Sand, the Journal of Canadian Petroleum Technology, Vol. 29, No. 2.

Edward, M., Braun, Robert, J., Blackwell, 1981. A Steady-State Technique for Measuring Oil-Water Relative Permeability Curves at Reservoir Conditions, SPE 10155.

Marcelo, M., 2005. Water-Oil Relative Permeability Comparative Study: Steady State versus Unsteady State, SCA-0577, presented at SCA Conference in Toronto, Canada.

Maloney, D.R., 2002. X-ray Imaging Technique Simplifies and Improves Reservoir-Condition Unsteady-State Relative Permeability Measurements, SCA-0211.

Naylor, P., Puckett, D., 1994. In-Situ Saturation Distributions: the Key to Understanding Core Analysis, SCA 9405.

Jones, S.C., Roszelle, W.O., 1978. Graphical Techniques for Determining Relative Permeability from Displacement Experiments, JPT. pp. 807-817.

Chen, A. L., Wood, A. C., 2001. Rate Effects on Water-Oil Relative Permeability, SCA-2001-19.

Craig, F.F., 1971. The Reservoir Engineering Aspects of Water-Flooding, Monograph Series, SPE, Richardson, TX 3.

Corey, A.T., 1954. The Interrelation Between Gas and Oil Relative Permeabilities, Prod. Monthly, Nov. 1954, PP.38-41.

Lomeland F., Ebeltoft E., Thomas W. H., 2005. A New Versatile Relative Permeability Correlation, SCA2005-32.